PHPMA. Grafting of the dendrimer by PHPMA decreases the toxicity of the dendrimer as well. Along this line, we previously reported that star-like HPMA copolymer, PHPMA-modified PAMAM dendrimer (SP-THP) conjugated with doxorubicin (DOX), showed superior tumor accumulation, and also antitumor activity to that of linear HPMA copolymer conjugates of DOX [5, 6]. Although previous star polymer-DOX conjugate showed high effectivity *in vivo*, a problem was that free DOX liberated from the conjugate exhibited slow intracellular uptake into tumor cells compared to free THP. Namely, it required about 100 times slower uptake time, probably it only depended on free diffusion mechanism. Consequently, slow uptake by tumor cells would result in wash out from the tumor site back into systemic circulation, followed by excretion from the body. Therefore, THP polymer conjugate would offer more advantage in *in vivo* setting, but not as much in *in vitro* culture cell system, and thus we have undertaken the present study.

In these polymer conjugates we utilized biodegradable linkers to attach the drug to the polymer [7, 8]. Advantage of using biodegradable linker is that the drug can be released from the polymer at or near the pathological region and then exhibits better therapeutic effect. One problem is connected with the use of some highly biocompatible polymer conjugates such as PEG or HPMA copolymer-conjugated drugs. They have lower intracellular uptake velocity than free drug, and consequently lower interaction with the target molecules resulting in lower therapeutic effect than one could expect [9-11]. Therefore, good release of low-MW drugs from the conjugates at tumor site is a critical issue for achieving the superior therapeutic effect, in order to exert drug action to the tumor [9]. For conjugating low-MW drugs, peptide, ester, disulfide and hydrazone bonds were used for conjugating the polymer and drugs [12, 13]. These chemical bonds can be cleaved by proteases and esterases which exist more dominantly in the tumor tissue. In addition, more acidic pH favors the spontaneous cleavage of hydrazone bond. Therefore, we designed conjugates with pH-controlled drug release taking place preferencially at the tumor tissue and at pathological lesions.

Here we describe the synthesis of SP-THP designed for efficient tumor accumulation due to the EPR effect of its macromolecular nature and we present results of the biological evaluation of novel dendrimer attached (star-like PHPMA copolymer conjugate of THP (SP-THP), in which surface of 2nd generation PAMAM (polyamido amine) dendrimer was grafted with chains of HPMA copolymers, which are conjugated with THP. For the detailed chemical structure of HPMA copolymer THP conjugate see [17]. THP was conjugated to the PHPMA via hydrazone bond, thus efficient drug release occur in the acidic environment of lysosomal pH and/or of tumor tissue. When we compared antitumor activity of SP-THP conjugate with linear HPMA copolymer-THP conjugate (LP-THP using two types of mouse tumor models, implanted and chemically induced tumor, we found superior tumor accumulation of SP-THP, and thus better therapeutic effect.

Materials and Methods

Materials

1-Aminopropan-2-ol, methacryloyl chloride, 4,4′-azobis(4-cyanovaleric acid) (ABIC), 6-aminohexanoic acid (ah), *N*,*N*′-dimethylformamide (DMF), *N*,*N*′-diisopropylcarbodiimide (DIPC), *N*-ethyldiisopropylamine (EDPA), dimethyl sulfoxide (DMSO), *tert*-butyl carbazate, trifluoroacetic acid (TFA) and 2,4,6-trinitrobenzene-1-sulfonic acid (TNBSA) were purchased from Sigma-Aldrich. Pirarubicin was purchased from Abbliss Chemicals, Houston, USA and poly(amido amine)

(PAMAM) dendrimers with 1,4-diaminobutane core were purchased from Dendritic Nanotechnologies, Inc., Atlanta, USA. Male ddY mice and ICR mice were purchased from Kyudo Co., Ltd, Saga, Japan. Dulbecco-MEM (DMEM) was purchased from Nissui Seiyaku, Tokyo, Japan. Azoxymethane, dextran sodium sulfate, and reagent grade salts were purchased from Wako Pure Chemical Industry, Osaka, Japan. 3-(4,5-Dimethyl-2-thiazolyl)-2,5-diphenyl-2H-tetrazolium bromide (MTT) was purchased from Dojindo Chemical Laboratories, Kumamoto, Japan. Fetal calf serum was purchased from Nichirei Bioscience, Tokyo, Japan.

Synthesis of monomers

N-(2-Hydroxypropyl)methacrylamide (HPMA) was synthesized as described in [14] using K_2CO_3 as a base. m.p. 70 °C; purity > 99.8 % (HPLC); elemental analysis: calc., C 58.72 %, H 9.15 %, N 9.78 %; found, C 58.98 %, H 9.18 %, N 9.82 %.

N-(*tert*-Butoxycarbonyl)-*N'*-(6-methacrylamidohexanoyl)hydrazine (Ma-ah-NHNH-Boc) was prepared in two-step synthesis as described in [15]. M.p. 110-114 °C; purity (HPLC) > 99.5 %; elemental analysis: calcd. C 57.70 C, H 8.33, N 13.46; found C 57.96, H 8.64, N 13.25. Purity of both monomers mentioned above was examined by HPLC (Shimadzu, Japan) using a reverse-phase column Chromolith Performance RP-18e 100-4.6 with PDA detection, eluent water–acetonitril with acetonitril gradient 0 – 100 vol.%, flow rate, 0.5 mL/min, and ^{1}H NMR Bruker spectrometer (300 MHz).

Synthesis of star-like polymer precursor

The star polymer precursor was prepared by grafting PHPMA with terminal thiazolidine-2-thione (TT) chain end group onto the 2nd generation PAMAM dendrimers containing terminal amino groups as described recently [16]. Briefly: Poly(HPMA-co-Ma-ah-NHNH-Boc) terminated with TT group (**copolymer I**) was prepared by radical solution copolymerization in DMSO initiated with azo-initiator ABIC-TT. Consequently, the star-like polymer precursor (Mw 256 000, Ð 2.1) was prepared by grafting the semitelechelic **copolymer I** onto PAMAM dendrimer (aminolysis of the copolymer TT group with amino groups of PAMAM in methanol). After 2 h, low-MW impurities were removed by gel filtration (Sephadex LH-20, solvent methanol) and the star hydrazide groups-containing polymer precursor (**copolymer II**) was isolated, after deprotection of the Boc protecting groups with concentrated TFA, by precipitation in ethyl acetate.

Synthesis of star polymer conjugate

The star polymer conjugate with pirarubicin attached via a pH-sensitive hydrazone bond was prepared by the reaction of the hydrazide groups-containing **copolymer II** with pirarubicin in methanol in the dark. After 18 h the conversion reached 98% (determined by HPLC in methanol/aqueous buffer solvent as described below) and the star polymer-drug conjugate was purified from low-Mw impurities (pirarubicin or its degradation products) by precipitation into ethylacetate. M_w = 400,000 g/mol; $Ð_n$ = 2.3, content of THP = 10.9 %wt; R_h= 13 nm. LP-THP was synthesised as describe before [17].

Cytotoxicity assay

HeLa cells (human cervical carcinoma) or B16-F10 cells (mouse melanoma) were maintained in DMEM supplemented with 10% fetal calf serum with 5% CO_2/air at 37 °C. HeLa cells were then incubated with SP-THP or LP-THP, or free THP for 72 h. The MTT assay was performed to quantify the cytotoxicity, with absorbance at 570 nm as usual.

Animal handling and evaluation of in vivo antitumor activity

The care and maintenance of animals were undertaken in accordance with the Institutional Animal Care and Use Committee of Sojo University.

S-180 tumor

Mouse sarcoma S-180 cells (2×10^6 cells) were implanted subcutaneously in the dorsal skin of ddY mice. When tumors became a diameter of about 4 mm, 5 or 15 mg/kg THP-equivalent drugs of SP-THP, LP-THP, or free THP in saline were injected intravenously (i.v.) at a volume of 0.2 mL per mouse. The tumor volume, body weight, and survival rate were recorded throughout the experiment period. The tumor volume (mm^3) was calculated as ($W^2 \times L$)/2 by measuring the length (L) and width (W) of the tumor on the dorsal skin.

AOM/DSS chemical induced colorectal tumor

Male ICR mice were administered i.p. injection of 10 mg/kg AOM (azoxymethan). One week after, mice were administered with 2% DSS p.o. for 1 week ad libitum. 10 weeks later, mice were randomly grouped, then 5 or 15 mg/kg THP-equivalent drugs in saline were injected i.v., 0.2 mL per mouse. Four weeks later, colon specimens were dissected, and number of tumor nodules and tumor area were calculated using ImageJ software.

Pharmacokinetics

S-180 tumor-bearing mice were administered 10 mg of THP equivalent/kg of LP-THP or SP-THP. At the indicated time periods, mice were killed, blood samples were withdrawn, and tissues were dissected after perfusion of the vascular void with physiological saline. Each tissue was homogenized by polytron homogenizer (Kinematica AG, Switzerland) after addition of PBS (900 μL/100 mg tissue). The amounts of total THP and released free THP in each tissue were measured as described previously [17].

Results
Physicochemical properties of SP-THP

SP-THP was synthesized as described in Materials and Methods. Apparent MW of each polymer conjugate was 400 kDa for SP-THP and 39 kDa for LP-THP respectively (Fig 1A). Loading of THP in SP-THP and LP-THP was 10.9 w/w % and 10.0 w/w % respectively. Hydrodynamic size of SP-THP in 10 mM phosphate buffered (pH 7.4) 0.15 M NaCl (PBS) was measured by dynamic light scattering, and found 25.9 ± 12.5 nm, which is larger than that of LP-THP (8.2 ± 1.7 nm) (Fig. 1B). Behavior of SP-THP in aqueous solution was also examined by size exclusion column chromatography on SB804-HQ column (SHODEX, tokyo). SP-THP was more quickly eluted than LP-THP, indicating that SP-THP behaved larger size molecule than LP-THP in aqueous solution (Fig. 1C).
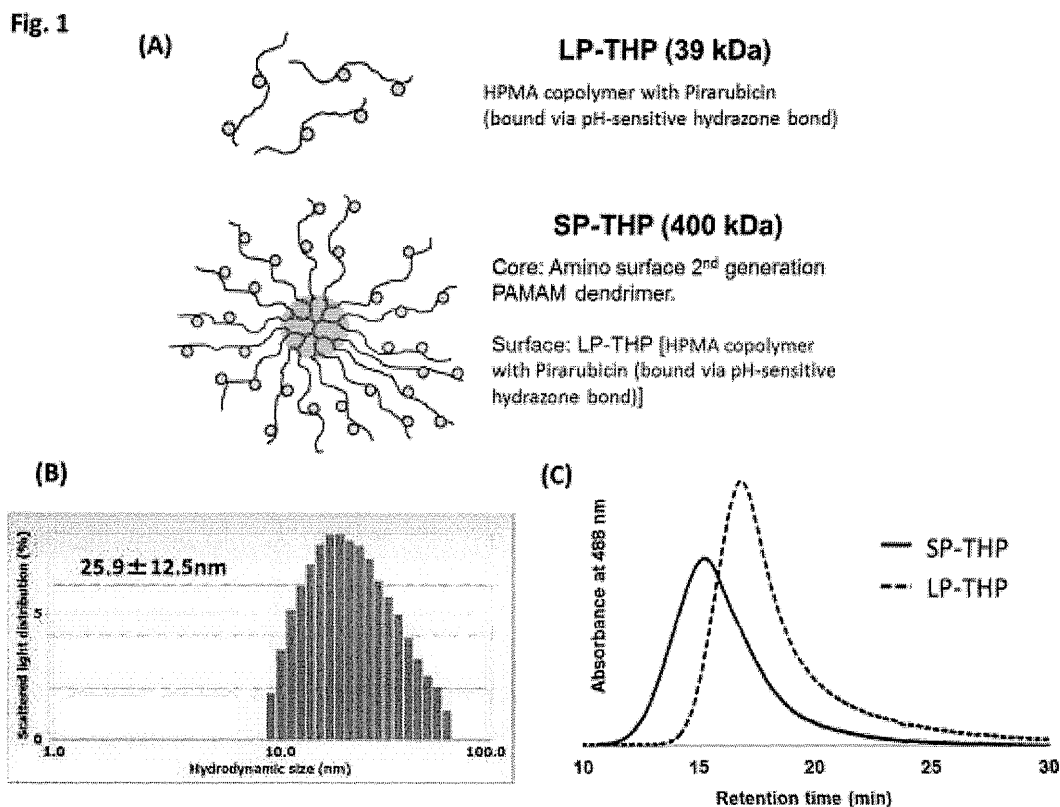
Fig. 1

(A)

LP-THP (39 kDa)

HPMA copolymer with Pirarubicin
(bound via pH-sensitive hydrazone bond)

SP-THP (400 kDa)

Core: Amino surface 2nd generation
PAMAM dendrimer.

Surface: LP-THP [HPMA copolymer
with Pirarubicin (bound via pH-sensitive
hydrazone bond)]

(B)

25.9±12.5nm

Scattered light distribution (%)

Hydrodynamic size (nm)

(C)

Absorbance at 488 nm

—— SP-THP
--- LP-THP

Retention time (min)

Fig. 1 Molecular size of SP-THP. (A) Illustrated image of LP-THP and SP-THP. (B) Hydrodynamic size of SP-THP dissolved in PBS at a concentration of 1 mg/mL was determined by dynamic light scattering (Otsuka Photal Electronics Co. Ltd., Osaka). (C) Size exclusion chromatography chromatograms of SP-THP and LP-THP using the column OHpak SB-804 HQ column (Showa Denko, Tokyo, Japan) (300 mm × 8.0 mm). Eluates were detected by photodiode array detector with absorbance at 488 nm.

Release of free THP

Cleavage of hydrazone bond, to release the free THP from SP-THP or LP-THP, was measured in aqueous solution in different pHs and we found that the release of THP from conjugates was pH dependent; 14 % was released in pH 7.4 and 88 % released in pH 5.0, both at 24h (Fig. 2). However, no significant difference in THP release was seen between SP-THP and LP-THP.
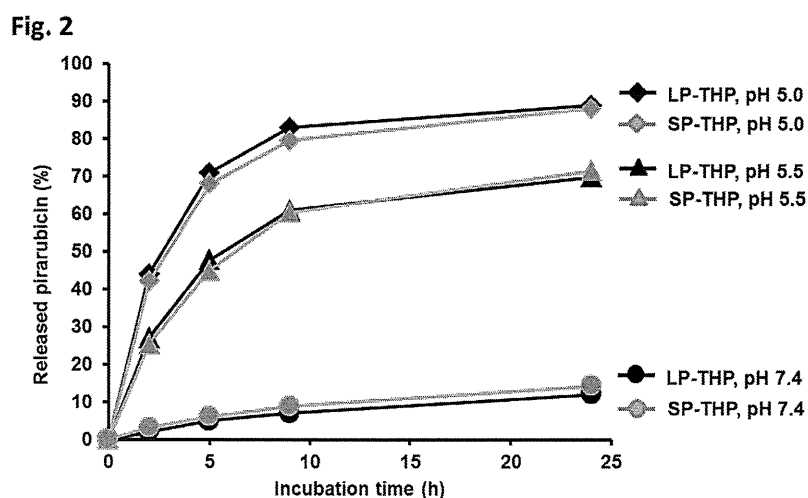
Fig. 2

Fig. 2. Release of free THP from SP-THP and LP-THP. SP-THP and LP-THP was incubated in 0.1 M phosphate buffer (with 0.05 M NaCl) at pH 5.0, 5.5 or 7.4 at 37 °C. At indicated time period, released THP was determined by HPLC.

Cytotoxicity of polymer THP conjugates

Cytotoxicity of SP-THP was examined using HeLa and B16/F10 cells in vitro, and found to be dose dependent. The cytotoxicity was 5 – 10 times lower than that of free THP. IC_{50} values of free THP, SP-THP, and LP-THP against HeLa cells were 0.08, 0.53, and 0.61µg/mL respectively (Fig. 3A). No remarkable difference in cytotoxicity was seen between SP-THP and LP-THP against both cell lines, HeLa and B16/F10 (Fig.3A and B).
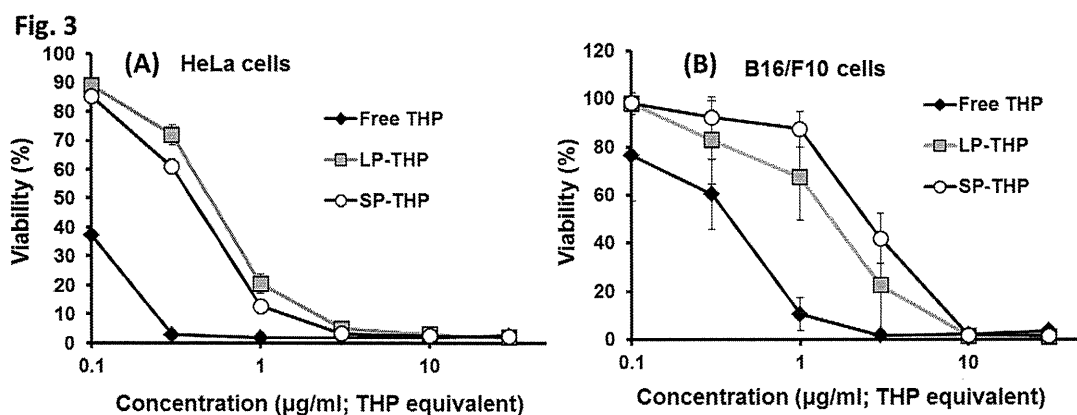
Fig. 3

Fig. 3. Cytotoxicity of SP-THP and LP-THP. (A) HeLa, or (B) B16/F10 cells were treated with indicated concentration of SP-THP, LP-THP, or free THP for 72h, then viable cells were measured by MTT assay. Viablility (%) in comparison with the non-treated control group was calculated. Values are mean ± S.D. Cytotoxicity of LP-THP and free THP was adapted from [17].

Pharmacokinetics of polymer-THP conjugates

Body distribution of SP-THP was examined in S-180 sarcoma mouse model. Ten mg/kg THP equivalent of SP-THP was injected i.v. at indicated time period. The level of THP as total

amount of THP (which was SP-THP and released free THP combined) and released free THP in each tissue was examined. At earlier time point than 24 h after i.v. administration, the highest total THP concentration was found in the plasma, and followed by tumor and then other normal organs (Fig. 4A (a)). However, as time passed, total THP concentration in tumor was slightly increased by EPR effect, in contrast to the decreasing concentration in plasma and in other normal organs (Fig. 4A). More interestingly, concentration of released free THP continued to increase in tumor up to 48 h after i.v. administration of SP-THP (Fig. 4B); released free THP concentration in tumor tissue was highest compared with all other normal tissues after 24 h up to 72 h (Fig. 4B). Tumor accumulation of SP-THP was approx 3 times higher than that of LP-THP (Fig. 4C).
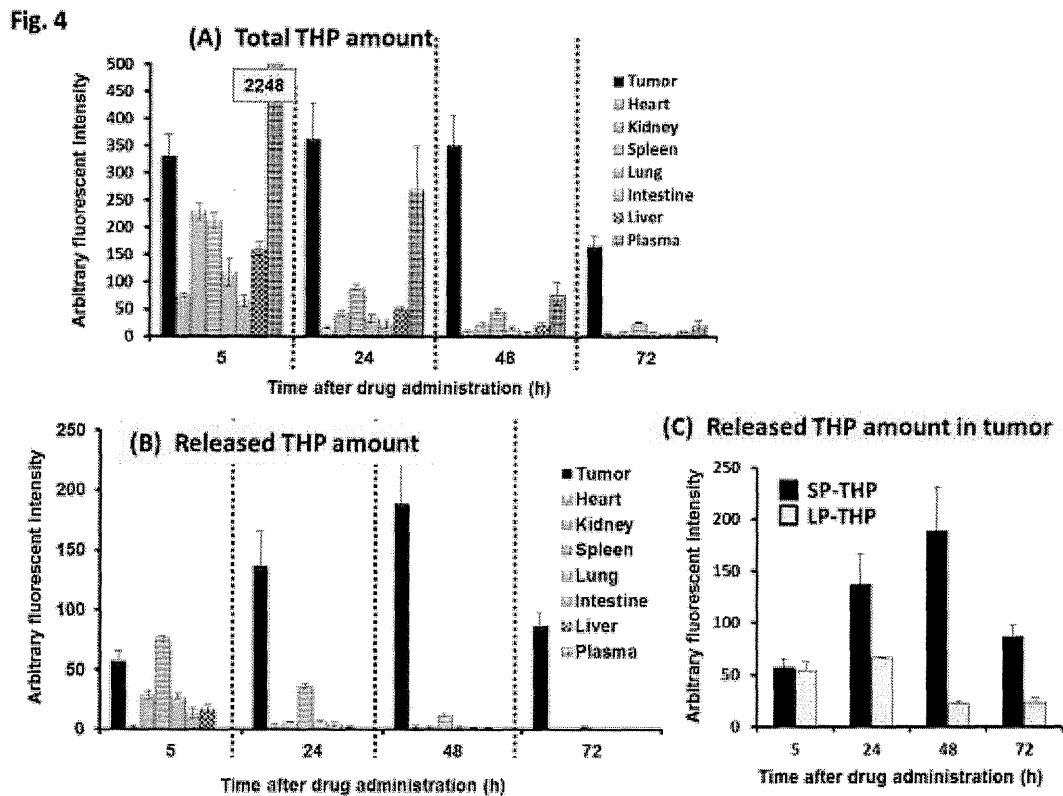

Fig. 4. Body distribution of SP-THP. (A) Amount of total THP (SP-THP + released THP), or (B) amount of released free THP in each tissues was detemined at indicated time intervals after drug admininistration. (C) Amount of released THP in the tumor after the treatment with SP-THP   or LP-THP (Values are means ± S.E. (n=3))

In vivo antitumor activity in S-180 tumor model

In the next experiment we examined *in vivo* antitumor activity of SP-THP against mouse sarcoma S-180, ectopically implanted tumor model. THP equivalent dose of SP-THP at 5 mg/kg was intravenously administered. Tumor in the non-treated control group was continued to grow, whereas, injection of SP-THP only once completely suppressed the tumor growth. Tumor suppression lasted at least up to 80 days after tumor inoculation. In contrast to the SP-THP, administration of LP-THP i.v. could not suppress tumor growth completely; tumor of one mouse out of five mice grew (Fig. 5).

Apparent body weight loss was not observed, at a dose of 5 mg/kg, in both SP-THP and LP-THP treated groups.
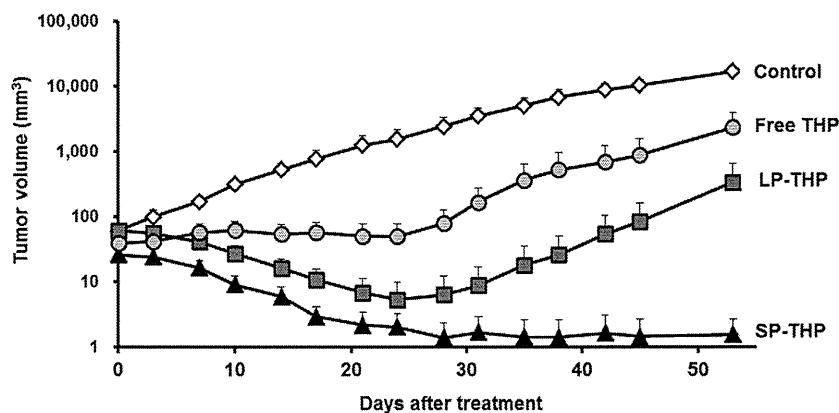
Fig. 5

Fig. 5. *In vivo* antitumor effect against S-180 tumor model. S-180 tumor bearing mice with tumor size of 5 – 6 mm was administered at a 5 mg/kg THP equivalent dose of free THP, LP-THP, and SP-THP. Values are means ± S.E. (n = 5 ~ 6)

In vivo antitumor activity of SP-THP in chemical AOM/DSS induced tumor model

Chemically induced tumor is more realistic model to clinical tumor than ectopically implanted tumor, especially regarding orthotopicity and autochthonous nature. The antitumor effect of SP-THP against chemical AOM (azoxymethane) / DSS (dextran sodium sulfate) induced colon tumor model is shown in SFig.1. Though administration of free THP or LP-THP did not suppress the tumor growth (number of tumor nodule and tumor area), 15 mg/kg THP equivalent dose of SP-THP clearly suppressed the tumor number and size (Fig. 6A and 6B). Slight body weight loss was observed in SP-THP treated group; though ~ 15 % (SFig.2).
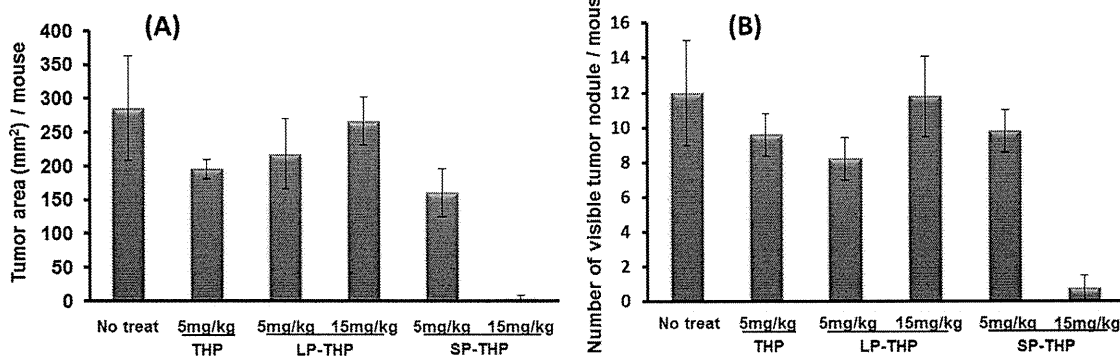
Fig. 6

Fig. 6. *In vivo* antitumor activity of SP-THP in the AOM / DSS induced colon tumor model. AOM / DSS induced colon tumor bearing mice were adminstered at a 5 – 15 mg/kg THP equivalent dose of free THP, LP-THP, and SP-THP. Four weeks later after treatment, colons were dissected, and tumor area (A) and number of tumor nodules (B) was calculated by using of ImageJ software. Values are means ± S.E. (n=5)

Discussion

Importance of free drug release at the target tissue, and its tumor cell uptake for achieving superior therapeutic effect are discussed elsewhere [18-20]. Therefore, biodegradable linkers such as peptide, ester, disulfide, acetal, and hydrazone etc. have been introduced between polymer carrier and therapeutic drugs [12]. In this study, we utilized the hydrazone linkage, which could be cleaved at the slightly acidic condition of tumor tissue. Hydrazone bond can be cleaved at the interstitial space of tumor tissue and intracellularly in lysosomes, thus, selective release of drug at the tumor tissue can be anticipated [16, 17]. Acid pH-labile hydrazone bond is useful for selective tumor drug release, because released active drug is the primary agent to show the therapeutic effect. Release profile of free THP from polymer conjugates, SP-THP and LP-THP, was examined, and found to be almost the same for both conjugates(Fig. 2). Essentially, THP was covalently bound to fully solvated PHPMA chain in both SP-THP and LP-THP via the same linkage, thus net MW of polymer conjugate might not affect the sensitivity to the hydrolysis of the hydrazone linkage.

As regards to the cytotoxicity (Fig. 3) and intracellular uptake (data not shown) of polymer conjugates, there was no remarkable difference between SP-THP and LP-THP. Considering these results, biological activity of SP-THP and LP-THP was almost similar at least in *in vitro* assay.

So, what was difference between SP-THP and LP-THP? Remarkable difference was in MW of SP-THP (400 kDa) and LP-THP (39 kDa) (Fig 1A). Hydrodynamic size of LP-THP and SP-THP was 8.2 nm and 25.9 nm respectively in aqueous solution (Fig. 1B). The larger hydrodynamic size of SP-THP was also confirmed by the size exclusion chromatography (Fig. 1C). These results clearly showed that SP-THP behaved much larger size than LP-THP in aqueous solution.

Molecular size of drugs has great impact on pharmacokinetics property and therapeutic effect [21, 22]. Most of small hydrophilic or hydrophobic molecules are quickly distributed in a whole body, and less accumulation of drugs could be observed in tumor or other lesions. In contrast, macromolecular drugs are retained longer in the systemic circulation, and they efficiently accumulate in the tumor tissue by the EPR effect. Moreover, macromolecules with larger size will accumulate more in the tumor tissue, rather than the macromolecules with smaller size [21, 22]. Therefore, pharmacokinetics of macromolecular drugs can be improved by increasing the size of macromolecular drugs. PHPMA modification of PAMAM dendrimer resulted in high-MW star-like PHPMA-based (SP) carrier (approx. 400 kDa) with narrow distribution, whereas LP-THP has MW of about 39kDa. In our previous study, DOX conjugated with SP (SP-DOX) exhibited better tumor accumulation and therapeutic effect than DOX conjugated with linear PHPMA (LP-DOX) in subcutaneous mice EL4 T-cell lymphoma model, indicating that SP carrier is preferable carrier for antitumor drugs to deliver them to the tumor tissue more efficiently [5, 6]. Recently we also showed that LP-THP exhibited the remarkable antitumor activity against S-180 subcutaneous tumor model [17].

Here we compared the antitumor activity of LP-THP and SP-THP in S-180 ectopically implanted tumor model and chemical AOM/DSS induced autochthonous tumor model.

Because of a larger size of SP-THP (25.9 nm, 400 kDa) in contrast to LP-THP (8.6 nm, 39 kDa), we anticipated that SP-THP would exhibit better pharmacokinetics, and thus antitumor effect. In S-180 tumor bearing mice, both LP-THP and SP-THP exhibited far preferable pharmacokinetic property than the conventional free THP. When we compared the LP-THP and SP-THP, tumor AUC (total THP; 5h ~ 72h) and AUC (released free THP; 5h ~ 72h) of SP-THP were 2.7 and 3.3 times higher than those of LP-THP respectively. More importantly, accumulation of released free THP (cytotoxic active drug) was only seen in the tumor tissue, especially 24 h after drug administration and not in any other normal organs (Fig. 4B). The data given above clearly showed that SP-THP was more selective toward tumor tissue. Because of higher tumor concentration of SP-THP, only single i.v. injection of 5 mg/kg THP equivalent dose of SP-THP was enough to suppress S-180 tumor growth completely; LP-THP and conventional free THP suppressed the tumor growth, however, the tumor gradually regrew. Antitumor activity of SP-THP was also examined using the chemical induced authocutonous tumor model. I.p. administration of AOM followed by p.o. administration of DSS causes colorectal tumor. This chemically induced tumor is more realistic tumor than ectopically inoculated tumor model, and it is difficult to treat. In such model, a single injection, however, of both conventional free THP and LP-THP could not suppress the tumor growth. In the case of SP-THP, dose of 15 mg/kg THP equivalent clearly suppressed the tumor growth; number of tumor nodule and tumor area was significantly decreased (Fig. 6). Unfortunately, slight body weight loss was seen (~15 %) in the SP-THP administration group (S. Fig 2), however, no mice died.   This might be because of released free THP in the systemic circulation, which would exert adverse effect. However, LD_{50} of parent free THP, LP-THP, and SP-THP were 14.2 mg/kg, 60 mg/kg, 23.4 mg/kg, respectively (S. Table 31). Both LP-TH and SP-THP conjugate showed lower toxicity and higher therapeutic efficacy than parent free THP (Fig. 5, S. Fig 3).   When both polymer THP conjugates were compared, SP-THP showed more potent toxicity (2 – 3 times) than LP-THP, indicating narrower therapeutic window. Although, the therapeutic efficacy of SP-THP was significantly higher than that of LP-THP, ultimate choice that which is better between the two for the clinical application is difficult, until the dose-limiting toxicity is clarified.

Conclusion

The present study describes the synthesis, physico-chemical characterization and the *in vivo* antitumor efficacy of the polymer conjugate SP-THP in comparison with the conjugate LP-THP and free THP. More remarkable accumulation of the high-MW conjugate SP-THP (400 kDa, 26nm) in the tumor tissue by EPR effect was observed than in case of LP-THP (39 kDa, 8.2nm). More importantly, SP-THP administration yielded more sustained release of free active THP for a long period of time in the tumor tissue even up to 72h. Thus SP-THP exhibited preferable antitumor effect against both S-180 and AOM/DSS induced colorectal tumor. Even single dose of 15 mg/kg THP equivalent clearly suppressed the tumor growth and prolonged the survival time. These results suggest that large size SP-THP conjugate is superior candidate drug for treatment of various solid tumors.

Acknowledgement

References

1. Tsukagoshi S. [Pirarubicin (THP-adriamycin)]. *Gan to kagaku ryoho Cancer & chemotherapy* 1988;15: 2819-27.

2. Seymour LW, Ulbrich K, Strohalm J, Kopecek J, Duncan R. The pharmacokinetics of polymer-bound adriamycin. *Biochemical pharmacology* 1990;39: 1125-31.

3. Seymour LW, Ulbrich K, Wedge SR, Hume IC, Strohalm J, Duncan R. N-(2-hydroxypropyl)methacrylamide copolymers targeted to the hepatocyte galactose-receptor: pharmacokinetics in DBA2 mice. *Br J Cancer* 1991;63: 859-66.

4. Noguchi Y, Wu J, Duncan R, Strohalm J, Ulbrich K, Akaike T, Maeda H. Early phase tumor accumulation of macromolecules: a great difference in clearance rate between tumor and normal tissues. *Jpn J Cancer Res* 1998;89: 307-14.

5. Etrych T, Kovar L, Strohalm J, Chytil P, Rihova B, Ulbrich K. Biodegradable star HPMA polymer-drug conjugates: Biodegradability, distribution and anti-tumor efficacy. *J Control Release* 2011;154: 241-8.

6. Etrych T, Strohalm J, Chytil P, Cernoch P, Starovoytova L, Pechar M, Ulbrich K. Biodegradable star HPMA polymer conjugates of doxorubicin for passive tumor targeting. *European journal of pharmaceutical sciences : official journal of the European Federation for Pharmaceutical Sciences* 2011;42: 527-39.

7. Azori M. Polymeric prodrugs. *Critical reviews in therapeutic drug carrier systems* 1987;4: 39-65.

8. Silva AT, Chung MC, Castro LF, Guido RV, Ferreira EI. Advances in prodrug design. *Mini reviews in medicinal chemistry* 2005;5: 893-914.

9. Malugin A, Kopeckova P, Kopecek J. Liberation of doxorubicin from HPMA copolymer conjugate is essential for the induction of cell cycle arrest and nuclear fragmentation in ovarian carcinoma cells. *J Control Release* 2007;124: 6-10.

10. Nakamura H, Liao L, Hitaka Y, Tsukigawa K, Subr V, Fang J, Ulbrich K, Maeda H. Micelles of zinc protoporphyrin conjugated to N-(2-hydroxypropyl)methacrylamide (HPMA) copolymer for imaging and light-induced antitumor effects in vivo. *J Control Release* 2013;165: 191-8.

11. Hatakeyama H, Akita H, Harashima H. The polyethyleneglycol dilemma: advantage and disadvantage of PEGylation of liposomes for systemic genes and nucleic acids delivery to tumors. *Biological & pharmaceutical bulletin* 2013;36: 892-9.

12. Fleige E, Quadir MA, Haag R. Stimuli-responsive polymeric nanocarriers for the controlled transport of active compounds: concepts and applications. *Adv Drug Deliv Rev* 2012;64: 866-84.

13. Zamboni WC. Concept and clinical evaluation of carrier-mediated anticancer agents. *Oncologist* 2008;13: 248-60.

14. Ulbrich K, Subr V, Strohalm J, Plocova D, Jelinkova M, Rihova B. Polymeric drugs based on conjugates of synthetic and natural macromolecules. I. Synthesis and physico-chemical characterisation. *J Control Release* 2000;64: 63-79.

15. Ulbrich K, Etrych T, Chytil P, Jelínková M, Říhová B. Antibody-targeted

polymer-doxorubicin conjugates with pH-controlled activation. *Journal of Drug Targeting* 2004;**12**: 477-89.

16. Etrych T, Jelinkova M, Rihova B, Ulbrich K. New HPMA copolymers containing doxorubicin bound via pH-sensitive linkage: synthesis and preliminary in vitro and in vivo biological properties. *J Control Release* 2001;**73**: 89-102.

17. Nakamura H, Etrych T, Chytil P, Ohkubo M, Fang J, Ulbrich K, Maeda H. Two mechanisms of tumor selective delivery of N-(2-hydroxypropyl)methacrylamide copolymer conjugated with pirarubicin via an acid-cleavable linkage. *J Control Release* 2013.

18. Maeda H. Macromolecular therapeutics in cancer treatment: the EPR effect and beyond. *J Control Release* 2012;**164**: 138-44.

19. Sezaki H, Hashida M. Macromolecule-drug conjugates in targeted cancer chemotherapy. *Critical reviews in therapeutic drug carrier systems* 1984;**1**: 1-38.

20. Ulbrich K, Subr V. Polymeric anticancer drugs with pH-controlled activation. *Adv Drug Deliv Rev* 2004;**56**: 1023-50.

21. Lo CL, Chou MH, Lu PL, Lo IW, Chiang YT, Hung SY, Yang CY, Lin SY, Wey SP, Lo JM, Hsiue GH. The effect of PEG-5K grafting level and particle size on tumor accumulation and cellular uptake. *International journal of pharmaceutics* 2013;**456**: 424-31.

22. Schadlich A, Caysa H, Mueller T, Tenambergen F, Rose C, Gopferich A, Kuntsche J, Mader K. Tumor accumulation of NIR fluorescent PEG-PLA nanoparticles: impact of particle size and human xenograft tumor model. *ACS nano* 2011;**5**: 8710-20.
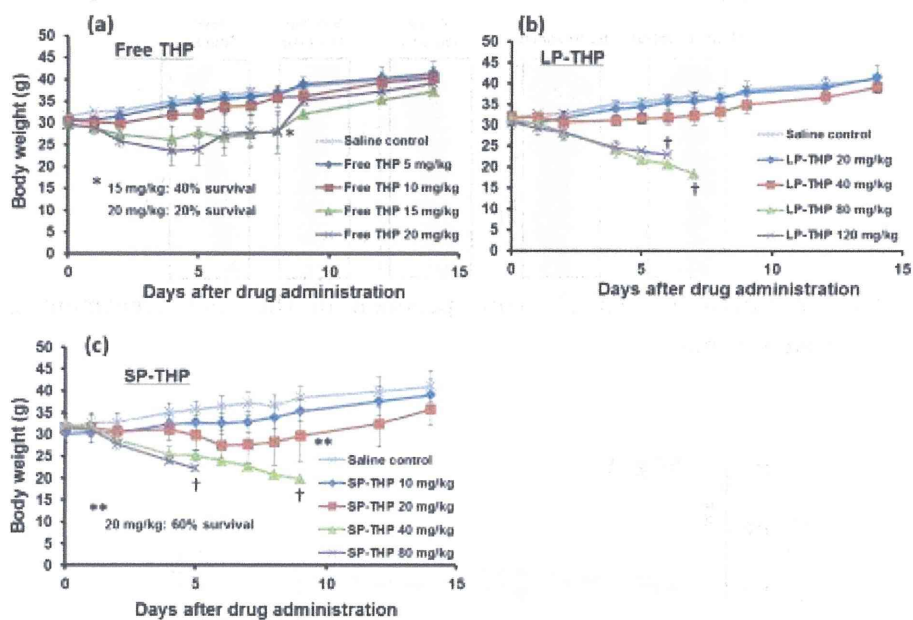
S. Fig. 1
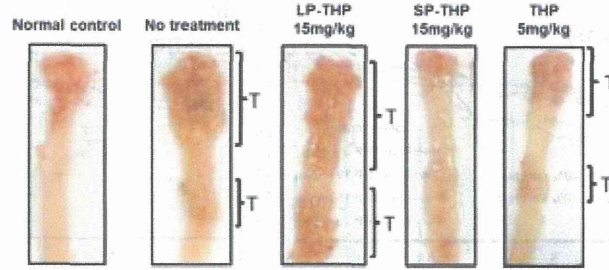
S. Fig.1. Representative images of colon specimen in the each treatment group. T indicates the area of tumor.
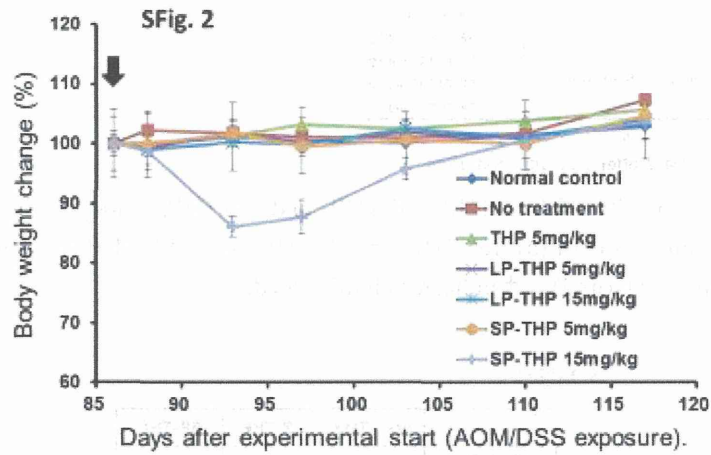
S. Fig. 2. Body weight change after drug administration. Body weights of mice were measured after administration of free THP, SP-THP, or LP-THP at an indicated dosage. Arrows indicates the timing of drug administration. Values are mean ± S.E. (n=5)

S. Fig. 3

S. Fig. 3. In vivo toxicity of free THP, LP-THP, and SP-THP. Body weights of mice were measured after administration of (a) free THP, (b) LP-THP, or (c) SP-THP at an one indicated dose iv. Values are mean ± S.D. (n=5). † indicates all mice died.

S. Table 1

	Free-THP	LP-THP	SP-THP
LD_{50} (mg/kg, THP equivalent)	14.2	60.0	23.4

S. Table 1. LD_{50} values of polymer THP conjugates in ddY mice (male) of 5 weeks old. LD_{50} values were calculated by method of Reed and Muench.

Tuning of Poly-S-Nitrosated Human Serum Albumin as Superior Antitumor Nanomedicine

YU ISHIMA,[1,2] JUN FANG,[3] ULRICH KRAGH-HANSEN,[4] HONGZHUAN YIN,[3] LONG LIAO,[3] NAOHISA KATAYAMA,[5] HIROSHI WATANABE,[1,2] TOSHIYA KAI,[6] AYAKA SUENAGA,[1] HIROSHI MAEDA,[7] MASAKI OTAGIRI,[1,3,7] TORU MARUYAMA[1,2]

[1] Department of Biopharmaceutics, Graduate School of Pharmaceutical Sciences, Kumamoto University, Kumamoto 862-0973, Japan
[2] Center for Clinical Pharmaceutical Science, Kumamoto University, Kumamoto 862-0973, Japan
[3] Faculty of Pharmaceutical Sciences, Sojo University, Kumamoto 860-0082, Japan
[4] Department of Biomedicine, University of Aarhus, Aarhus CDK-8000, Denmark
[5] Pharmaceutical Research Laboratories, Kusatsu, Shiga 525-0055, Japan
[6] Tohoku Nipro Pharmaceutical Corporation, Kagamiishimachi, Iwasegun, Fukushima 969-0401, Japan
[7] Drug Delivery System Institute, Sojo University, Kumamoto 860-0082, Japan

ABSTRACT: Macromolecules have been developed as carriers of low-molecular-weight drugs in drug delivery systems (DDS) to improve their pharmacokinetic profile or to promote their uptake in tumor tissue via enhanced permeability and retention (EPR) effects. We have previously demonstrated that poly-nitric oxide (NO) conjugated human serum albumin (Poly-SNO-HSA) has the potential to be a DDS carrier capable of accumulating NO in tumors. However, the stability of Poly-SNO-HSA in the circulation has to be improved, and its optimal molecular size for using the EPR effects has to be evaluated. In the present study, we performed two tuning methods for refining Poly-SNO-HSA, namely, pegylation and dimerization. We observed that pegylation enhanced the stability of Poly-SNO-HSA both *in vitro* and *in vivo*, and that dimerization of Poly-SNO-HSA enhanced the antitumor activity via more efficient delivery of NO in Colon 26 tumor-bearing mice. Intriguingly, dimerization resulted in a 10 times higher antitumor activity. These data suggest that pegylation and dimerization of Poly-SNO-HSA are very important tuners to optimize NO stability and accumulation, and thereby effect, in tumors. Thus, polyethylene glycol-Poly-SNO-HSA dimer seems to be a very appealing and safe NO carrier and thereby a strong candidate as an antitumor drug in future development of cancer therapeutics. © 2014 Wiley Periodicals, Inc. and the American Pharmacists Association J Pharm Sci
Keywords: human serum albumin; nitric oxide; drug delivery system; antitumor activity; pegylation; dimerization; cancer; controlled release/delivery; macromolecular drug delivery; nanoparticles

INTRODUCTION

Cancer treatment remains one of the most important clinical challenges. One problem in treating various cancers is the development of multidrug resistance (MDR) by the cancer cells. Various approaches have been tested to overcome MDR such as the use of agents that inhibit P-glycoprotein directly or indirectly through altering the cell membrane. Most of the approaches have shown some success in small animal models but their clinical application has been limited. Because nitric oxide (NO) seems to be able to overcome MDR, and has other promising properties and effects, it has the potential of becoming a useful anticancer therapeutic.[1,2]

Nitric oxide is a free-radical gas involved in diverse biological processes, such as neurotransmission, blood pressure control, inhibition of platelet aggregation, and innate immunity.[3] However, under certain circumstances, NO can be cytotoxic. For example, high concentrations of NO can inhibit tumor cell growth and induce apoptosis.[4,5] Recent studies have revealed that NO is associated not only with apoptosis of cancer cells,

but also with inhibition of cancer progression and metastasis, as well as cancer angiogenesis and microenvironment. It also functions as a modulator for chemo/radio/immunotherapy.[6] Despite highly useful properties, the *in vivo* half-life of NO is so short that NO itself cannot be used as a therapeutic agent. Such a short half-life can be overcome using continuous release of NO from a reservoir, such as the S-nitrosated form of human serum albumin (HSA).[7–9]

Our previous studies with cell cultures demonstrated that the NO influx from poly-nitric oxide conjugated human serum albumin (Poly-SNO-HSA) via cell surface protein disulfide isomerase is very fast and pronounced and leads to cell death caused by apoptosis. However, the apparent *in vivo* half-life of S-nitroso moieties in Poly-SNO-HSA has been estimated to be 18.9 min in tumor-bearing rats, indicating that it is not always a long-acting medicine.[10] Therefore, the release rate of NO from Poly-SNO-HSA needs to be well controlled and prolonged to develop more effective NO delivery systems. Shishido and de Oliveira[11] have shown that the thermal stability of S-nitrosothiols is increased in polyethylene glycol (PEG) solution because the cage effect of PEG increased the stability of S–NO bonding. Perhaps, this effect can be applied to construct more useful Poly-SNO-HSA preparations.

In addition to *in vivo* half-life, the problem of drug targeting should be addressed. In this respect, the enhanced permeability

and retention (EPR) effect is relevant. This effect is now known to play a major role in the tumor-selective delivery of macromolecular or polymeric drugs, or of so-called nanomedicines including antibodies.[12–14] It is well known that long-circulating liposomes with an average diameter of 100–200 nm accumulate efficiently in tumor tissues.[15] Matsumura and Maeda[16] found that high-molecular-weight (40 kDa or higher), long-circulating macromolecules, as well as various long-circulating nanoparticulate pharmaceutical carriers are capable of spontaneously accumulating in various pathological sites, such as solid tumors and infracted areas. However, recently, Kataoka's group demonstrated that only 30-nm micelles could penetrate poorly permeable pancreatic tumors to achieve an antitumor effect.[17] These data suggest that macromolecular therapeutics with a size of 30 nm could efficiently deliver to even poorly permeable tumors. For testing this possibility, we have designed a HSA dimer, in which the C-terminus of one HSA molecule is linked to the N-terminus of another HSA molecule by the amino acid linker (GGGGS)$_2$, that can be successfully produced by the yeast *Pichia pastoris*. We have previously reported that HSA dimer has a longer circulation time than the monomeric form of HSA, HSA monomer, in rats and mice.[18] Moreover, HSA dimer could have an enhanced accumulation in solid and poorly permeable tumors via the EPR mechanism because of its molecular size of approximately 30 nm (130 kDa). Therefore, it is possible that HSA dimer could be of great clinical use as a new DDS material with a superior plasma retention property (e.g., prolonged plasma half-life) as well as with increased tumor-specific accumulation.

In this study, we performed two tuning methods of pegylation and dimerization of Poly-SNO-HSA. We examined the effect of pegylation on the stability of *S*-nitrosated sites of Poly-SNO-HSA *in vitro* and *in vivo*, and the effect of dimerization of Poly-SNO-HSA on its antitumor activity in Colon 26 (C26) tumor-bearing mice.

MATERIALS AND METHODS

Materials

Human serum albumin and HSA dimer were synthesized using the yeast *Pichia pastoris* (*P. pastoris*) (strain GS115) as previously described,[18] and the proteins were defatted by means of charcoal treatment.[19] Sephadex G-25 desalting column (ϕ 1.6 × 2.5 cm) was obtained from GE Healthcare (Kyoto, Japan). 1,4-dithiothreitol was obtained from Sigma–Aldrich (St. Louis, Missouri). Isopentyl nitrite (IAN) was bought from Wako Chemicals (Osaka, Japan). Diethylenetriaminepentaacetic acid (DTPA) and ethylenediaminetetraacetic acid were purchased from Nacalai Tesque (Kyoto, Japan). $^{111}InCl_3$ was a gift from Nihon Medi-Physics Company, Ltd. (Hyogo, Japan).

Cells and Animals

C26 cells were cultured in RPMI-1640 containing 10% fetal bovine serum (Sanko Junyaku Co, Ltd.,Tokyo, Japan), 100 units/mL penicillin, and 100 µg/mL streptomycin, incubated in a humidified (37°C, 5% CO_2 and 95% air) incubator, grown in 75-cm^2 flasks (Falcon BD) Tokyo, Japan, and passaged when 75% confluency was reached. Male BALB/cAnNCrlCrlj mice (5 weeks old, 17–22 g) were purchased from Charles River Laboratories (Ibaraki, Japan). A C26 solid tumor model was established by subcutaneously implanting 2 × 10^6 C26 cells into

the back of the mice. Other animals, that is, male ddY mice and male Donryu rats, were from Kyudo Inc. (Kumamoto, Japan).

Pegylation and *S*-Nitrosation

To perform the pegylation of HSA, HSA–polyethylene glycol conjugate-5000 (PEG–HSA) was synthesized by reacting activated PEG with HSA in 50 mM borate buffer (pH 9.2) for 24 h at 4°C in the dark to react with available amino acids.[20] The reaction mixture was then washed and concentrated by ultrafiltration against distilled water. The average number of PEG moieties is 4.6 mol PEG/mol HSA, and the molecular weight of the product is estimated to be 90 kDa by using SDS-PAGE (data not shown).

Poly-nitric oxide conjugated human serum albumins were prepared according to a previous report.[4] In brief, terminal sulfhydryl groups were added to HSA, PEG–HSA, and HSA dimer by incubating 0.15 mM HSA, 0.15 mM PEG–HSA or 0.075 mM HSA dimer with 3 mM Traut's Reagent (2-imminothiolane) in 100 mM potassium phosphate buffer containing 0.5 mM DTPA (pH 7.8) for 1 h at 25°C. The resultant modified HSA, PEG–HSA, and HSA dimer was then *S*-nitrosated by 3 h incubation with 15 mM IAN at 25°C. The resulting Poly-SNO-HSA, PEG-Poly-SNO-HSA, or Poly-SNO-HSA dimer was concentrated, exchanged with saline using a PelliconXL filtration device (Millipore Corporation, Billerica, Massachusetts), and the final concentration was adjusted to 2 mM Poly-SNO-HSA, 2 mM PEG-Poly-SNO-HSA, or 1 mM Poly-SNO-HSA dimer. The samples were stored at 80°C until use . The number of NO moieties bound to Poly-SNO-HSA and PEG-Poly-SNO-HSA is 6.7 mol NO/mol protein, whereas the number bound to Poly-SNO-HSA dimer is 13.5 mol NO/mol protein.

Pharmacokinetic Experiments

Poly-nitric oxide conjugated human serum albumin was labeled with ^{111}In by using DTPA anhydride as a bifunctional chelating agent.[21] Labeled Poly-SNO-HSA was injected via the tail vein into male ddY mice (weighing 25–27 g) at a dose of 5 µmol NO/kg. At appropriate times after injection, blood was collected from the vena cava with the mouse under ether anesthesia. Heparin sulfate was used as an anticoagulant, and plasma was obtained from the blood by centrifugation. The radioactivity in each sample was counted using a well-type NaI scintillation counter ARC-2000 (Aloka, Tokyo, Japan). ^{111}In radioactivity concentrations in plasma were normalized as a percentage of the dose injected per milliliter and were analyzed by means of the nonlinear least-squares program MULTI.[22] We also measured the amount of *S*-nitrosated moieties in the plasma samples. That was performed by means of the Saville assay.[23]

Effect of Pegylation on the Stability of S-Nitrosated Sites of Poly-SNO-HSA

For *in vitro* study, Poly-SNO-HSA or PEG-Poly-SNO-HSA at a NO concentration of 100 µM was incubated in mouse blood or plasma at 37°C for different times in the dark. For *in vivo* study, Poly-SNO-HSA or PEG-Poly-SNO-HSA at doses of 5 µmol NO/kg were injected as a bolus through the tail vein of 5-week-old male Donryu rats (200–250 g), and NO concentrations in plasma were determined at 1, 15, 30, 60, 180, and 360 min after injection. The amounts of the *S*-nitrosated moieties of Poly-SNO-HSA and PEG-Poly-SNO-HSA were quantified using a 96-well plate. First, 20 µL aliquots of Poly-SNO-HSA or

Table 1. Pharmacokinetic Parameters for HSA and NO After Intravenous Administration (5 µmol/kg) of Poly-SNO-HSA to Normal Mice

	AUC_{0-4} (mM min)	CL_{tot} (mL/min/kg)	$t_{1/2\beta}$ (min)	V_1 (mL/kg)
HSA	52.10 ± 6.56	0.10 ± 0.05	476.6 ± 12.6	60.10 ± 4.35
NO moieties	11.17 ± 4.43	2.87 ± 0.75	118.7 ± 11.8	75.47 ± 6.54

All values are mean $\pm$ SD ($n = 5$).

PEG-Poly-SNO-HSA solution and $NaNO_2$ (standard) were incubated for 30 min at room temperature with 0.2 mL of 10 mM sodium acetate buffer (pH 5.5) containing 100 mM NaCl, 0.5 mM DTPA, 0.015% N-1-naphthylsthylene-diamide, and 0.15% sulfanilamide with or without 0.09 mM $HgCl_2$. Then, the absorbance was measured at 540 nm.[23]

Antitumor Study *In Vivo*

When tumors reached 150–200 mm³, the mice were divided into cohorts ($n = 4$–5), and 200 µL saline (control); Poly-SNO-HSA (5 or 25 mg/mouse) or Poly-SNO-HSA dimer (0.5 or 2.5 mg/mouse) was injected via the tail vein three times per day on days 0, 2, and 4.[4] Afterwards, tumor volume and body weight were determined every day for 25 days. Tumor volume was calculated using the formula 0.4 (a × b²), where "a" is the largest and "b" is the smallest tumor diameter. After 25 days, blood samples were collected from the abdominal vena cava under anesthesia with diethylether of the mice that had received saline, Poly-SNO-HSA (25 mg/mouse), or Poly-SNO-HSA dimer (2.5 mg/mouse). Afterwards, the mice were sacrificed. Serum was isolated by centrifugation. Routine clinical laboratory techniques were used to determine the concentrations of total protein, serum creatinine (Cr), blood urea nitrogen (BUN), alanine aminotransferase (ALT), aspartate aminotransferase (AST), and alkaline phosphatase (ALP) in serum. Variance in each group was evaluated using the Bartlett test, and differences were evaluated using the Tukey–Kramer test.

Statistical Analysis

The statistical significance of collected data was evaluated using the ANOVA analysis followed by Newman–Keuls method for more than two means. Differences between the groups were evaluated by Student's t-test. $p < 0.05$ was regarded as statistically significant.

RESULTS AND DISCUSSION

Plasma Clearance of HSA and NO After Poly-SNO-HSA Administration

We determined the pharmacokinetic characteristics of both HSA and the NO moieties of Poly-SNO-HSA after its injection into normal male ddY mice (Table 1). As seen in Figure 1, the plasma concentration of the NO moieties decreases much more rapidly than that of HSA. In accordance with this finding, the half-life ($T_{1/2\beta}$) for HSA was calculated to be 477 min, whereas that for the NO moieties was only 119 min (Table 1). These data propose that the SNO stability of Poly-SNO-HSA is very low in the circulation.
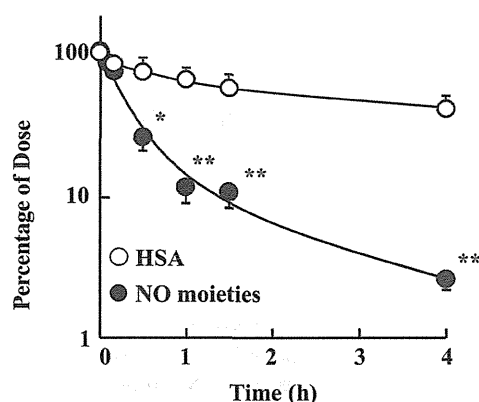
Figure 1. Plasma clearance of HSA and NO after intravenous administration (5 µmol/kg) of Poly-SNO-HSA to normal mice. Poly-SNO-HSA was injected as a bolus through the tail vein of mice, and HSA and NO concentrations in plasma are plotted against time after injection. Each datum point represents the mean $\pm$ SD. ($n = 5$). *$p < 0.05$, **$p < 0.01$ as compared with HSA.

In Vitro and *In Vivo* Release of NO from Poly-SNO-HSA and PEG-Poly-SNO-HSA

In an attempt to develop a more stable NO delivery system, we constructed pegylated Poly-SNO-HSA (PEG-Poly-SNO-HSA). First, we compared the stability of Poly-SNO-HSA and PEG-Poly-SNO-HSA in blood and plasma from normal mice at 37°C in the dark. Figure 2a shows that PEG-Poly-SNO-HSA is very stable as compared with Poly-SNO-HSA in blood. The half-life of PEG-Poly-SNO-HSA is 2.5 times longer than that of Poly-SNO-HSA. By contrast, there is no difference in stability between the two SNO preparations in plasma. The results suggest that S-denitrosation of Poly-SNO-HSA by other plasma proteins is insignificant and unaffected by pegylation.

For making an *in vivo* study of the NO release from Poly-SNO-HSA and PEG-Poly-SNO-HSA, we injected aliquots of the two protein preparations as a bolus through the tail vein of rats. As seen in Figure 2b, NO bound to the pegylated protein disappears more slowly from the circulation than does NO bound to the unpegylated protein; the NO half-lives are 155 and 105 min, respectively. Thus, both this study and that performed with mouse blood (Fig. 2a) shows that pegylation is a very useful way of SNO stabilization in the case of Poly-SNO-HSA.

Effect of Dimerization on the Antitumor Activity of Poly-SNO-HSA

One way of making cancer treatment more efficient is to increase the concentration of the therapeutic in the tumor. Such an increase in concentration can be obtained as the result of the EPR effect. For testing whether an increase in protein size would result in a more efficient EPR effect, we synthesized an albumin dimer that we also S-nitrosated, that is, Poly-SNO-HSA dimer. Figure 3a shows the antitumor activity of Poly-SNO-HSA dimer in mice compared with that of Poly-SNO-HSA. As seen, both albumin therapeutics have an inhibitory effect on tumor growth. However, Poly-SNO-HSA dimer possesses about at least 10 times higher antitumor activity than Poly-SNO-HSA.

In general, the body weights of the mice increased with reduction of tumor volume (Fig. 3b). An exception is the group of
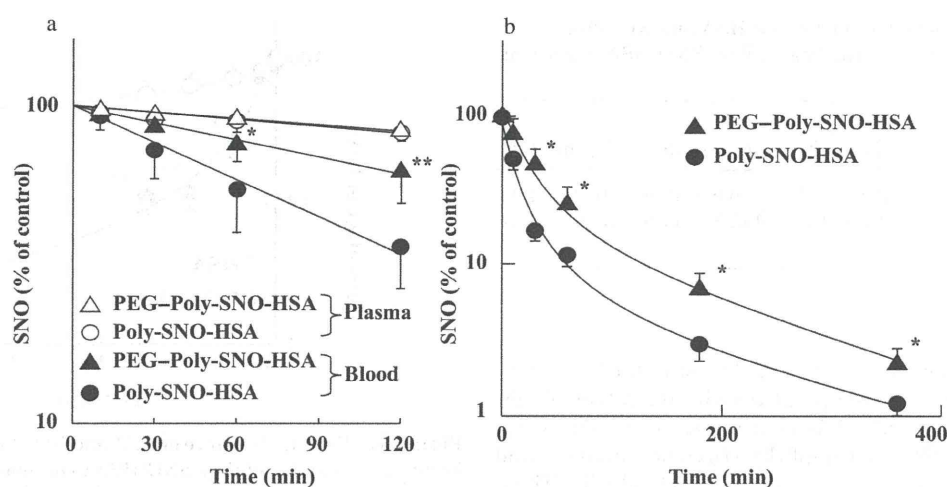
Figure 2. Time course for NO decay when incubated in blood or plasma (a) and plasma clearance of NO after intravenous administration of Poly-SNO-HSA or PEG-Poly-SNO-HSA (b). Poly-SNO-HSA or PEG-Poly-SNO-HSA at the concentration of 100 μM was incubated in mouse blood or plasma at 37°C for the indicated time in the dark. Each datum point represents the mean ± SD for three experiments. $*p < 0.05$, $**p < 0.01$ as compared with Poly-SNO-HSA in blood. Poly-SNO-HSA or PEG-Poly-SNO-HSA (5 μmol/kg) was injected as a bolus through the tail vein of rats, and NO concentrations in plasma are plotted against time after injection. $*p < 0.05$ as compared with Poly-SNO-HSA.
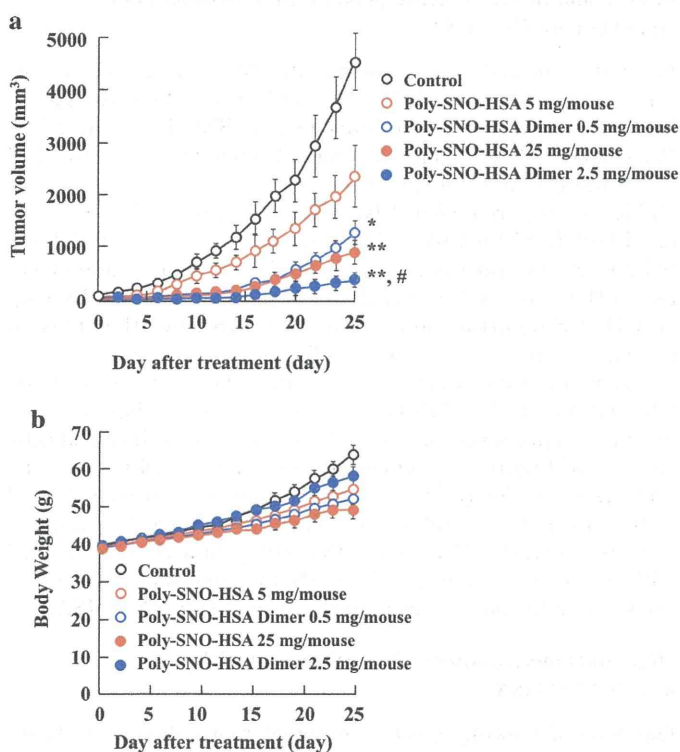
Figure 3. Effect of Poly-SNO-HSA and Poly-SNO-HSA dimer on tumor growth (a) and body weight (b) of C26 tumor-bearing mice. The C26 tumor-bearing mice were divided into cohorts ($n = 4$–5), and saline (control) or Poly-SNO-HSA (5 or 25 mg/mouse) or Poly-SNO-HSA dimer (0.5 or 2.5 mg/mouse) was injected three times per day on days 0, 2, and 4 via the tail vein. Results are for the following 25 days and are given as means ± SD. $*p < 0.05$, $**p < 0.01$ as compared with control. $#p < 0.05$ as compared with Poly-SNO-HSA (25 mg/mouse).

mice that each received 2.5 mg of Poly-SNO-HSA dimer. Their body weight increased more than expected, a finding suggest-

ing that these mice may recover very well and fast from the hypophagia associated with the colon cancer.

Table 2 shows values of serum biochemical parameters of the C26 tumor-bearing mice treated with saline, Poly-SNO-HSA, or Poly-SNO-HSA dimer. As seen, total protein and serum creatinine (Cr) showed no significant differences among the three treated groups. However, BUN, AST, ALT, and ALP significantly decreased by Poly-SNO-HSA dimer treatment, indicating that Poly-SNO-HSA dimer did not cause hepatic or renal damage. In general, ALP levels increase in several types of cancer, such as liver, lung, and bone cancer, whereas the present finding indicates that Poly-SNO-HSA dimer protects against various organ damage induced by the tumor. Thus, the present findings suggest that Poly-SNO-HSA dimer is an effective and safe anticancer agent.

CONCLUSIONS

Previous studies have shown that Poly-SNO-HSA possesses antitumor activity *in vivo*. However, the SNO groups of Poly-SNO-HSA have low stability in the circulation, and high dosages of Poly-SNO-HSA cause reduction in the mean arterial blood pressure.[9] In this paper, we performed two tuning methods of Poly-SNO-HSA, namely, pegylation and dimerization. We found that pegylation enhances the stability of the *S*-nitrosated sites of Poly-SNO-HSA both *in vitro* and *in vivo*. Furthermore, dimerization of Poly-SNO-HSA resulted in improved antitumor activity via more efficient delivery of NO in C26 tumor-bearing mice. In addition, as an antitumor nanomedicine, PEG-Poly-SNO-HSA dimer possesses an important high biocompatibility and biodegradability. These findings lead to the idea that PEG-Poly-SNO-HSA dimer possesses the clinical possibility for being a superior and promising anticancer drug with reduction of side effects.

ACKNOWLEDGMENTS

Table 2. Serum Biochemical Parameters of Control Mice and C26 Tumor-Bearing Mice Treated with Saline, Poly-SNO-HSA, or Poly-SNO-HSA Dimer

	Control Mice (Not Tumor-Bearing Mice)	Saline	Poly-SNO-HSA (25 mg/mouse)	Poly-SNO-HSA Dimer (2.5 mg/mouse)
Total protein (g/dL)	5.35 ± 0.35	5.23 ± 0.21	5.55 ± 0.24	5.32 ± 0.20
Cr (mg/dL)	0.10 ± 0.07	0.13 ± 0.04	0.16 ± 0.01	0.14 ± 0.01
BUN (mg/dL)	18.6 ± 2.76	15.25 ± 0.96	13.75 ± 1.26	12.45 ± 0.76*
AST (U/L)	67.7 ± 12.9	143.5 ± 62.9	116.3 ± 69.1	102.1 ± 63.7*
ALT (U/L)	39.7 ± 13.6	169.8 ± 111.6	161.3 ± 126.2	101.1 ± 108.7**,##
ALP (U/L)	329.1 ± 23.3	385.3 ± 18.3	300.5 ± 23.0**	276.5 ± 21.2**,#

All values are mean ± SD (n = 4–5).
*$p < 0.05$, **$p < 0.01$, versus saline; #$p < 0.05$, ##$p < 0.01$ versus Poly-SNO-HSA.

REFERENCES

1. Ishima Y, Hara M, Kragh-Hansen U, Inoue A, Suenaga A, Kai T, Watanabe H, Otagiri M, Maruyama T. 2012. Elucidation of the therapeutic enhancer mechanism of poly-S-nitrosated human serum albumin against multidrug-resistant tumor in animal models. J Control Release 164:1–7.
2. Park K. 2012. Poly-SNO-HSA: A safe and effective multifunctional antitumor agent. J Control Release 164:105.
3. Moncada S, Palmer RM, Higgs EA. 1991. Nitric oxide: Physiology, pathophysiology, and pharmacology. Pharmacol Rev 43:109–142.
4. Katayama N, Nakajou K, Komori H, Uchida K, Yokoe J, Yasui N, Yamamoto H, Kai T, Sato M, Nakagawa T, Takeya M, Maruyama T, Otagiri M. 2008. Design and evaluation of S-nitrosolated human serum albumin as novel anticancer drug. J Pharmacol Exp Ther 325:69–76.
5. Ishima Y, Yoshida F, Kragh-Hansen U, Watanabe K, Katayama N, Nakajou K, Akaike T, Kai T, Maruyama T, Otagiri M. 2011. Cellular uptake mechanisms and responses to NO transferred from mono- and poly-S-nitrosated human serum albumin. Free Radic Res 45:1196–1206.
6. Ishima Y, Kragh-Hansen U, Maruyama T, Otagiri M. 2013. Poly-S-nitrosated albumin as a safe and effective multifunctional antitumor agent: Characterization, biochemistry and possible future therapeutic applications. Biomed Res Int 2013:353892.
7. Marley R, Feelisch M, Holt S, Moore K. 2000. A chemiluminescense-based assay for S-nitrosoalbumin and other plasma S-nitrosothiols. Free Radic Res 32:1–9.
8. Marks DS, Vita JA, Folts JD, Keaney JF Jr, Welch GN, Loscalzo J. 1995. Inhibition of neointimal proliferation in rabbits after vascular injury by a single treatment with a protein adduct of nitric oxide. J Clin Invest 96:2630–2638.
9. Katsumi H, Nishikawa M, Yamashita F, Hashida M. 2005. Development of polyethylene glycol-conjugated poly-S-nitrosated serum albumin, a novel S-Nitrosothiol for prolonged delivery of nitric oxide in the blood circulation in vivo. J Pharmacol Exp Ther 314:1117–1124.
10. Katayama N, Nakajou K, Ishima Y, Ikuta S, Yokoe J, Yoshida F, Suenaga A, Maruyama T, Kai T, Otagiri M. 2010. Nitrosylated human

serum albumin (SNO-HSA) induces apoptosis in tumor cells. Nitric Oxide 22:259–265.
11. Shishido SM, de Oliveira MG. 2000. Polyethylene glycol matrix reduces the rates of photochemical and thermal release of nitric oxide from S-nitroso-N-acetylcysteine. Photochem Photobiol 71:273–280.
12. Maeda H, Sawa T, Konno T. 2001. Mechanism of tumor-targeted delivery of macromolecular drugs, including the EPR effect in solid tumor and clinical overview of the prototype polymeric drug SMANCS. J Control Release 74:47–61.
13. Maeda H, Wu J, Sawa T, Matsumura Y, Hori K. 2000. Tumor vascular permeability and the EPR effect in macromolecular therapeutics: A review. J Control Release 65:271–284.
14. Maeda H. 2001. SMANCS and polymer-conjugated macromolecular drugs: Advantages in cancer chemotherapy. Adv Drug Deliv Rev 46:169–185.
15. Yuan F, Leunig M, Huang SK, Berk DA, Papahadjopoulos D, Jain RK. 1994. Microvascular permeability and interstitial penetration of sterically stabilized (stealth) liposomes in a human tumor xenograft. Cancer Res 54:3352–3356.
16. Matsumura Y, Maeda H. 1986. A new concept for macromolecular therapeutics in cancer chemotherapy: Mechanism of tumoritropic accumulation of proteins and the antitumor agent SMANCS. Cancer Res 46:6387–6392.
17. Cabral H, Matsumoto Y, Mizuno K, Chen Q, Murakami M, Kimura M, Terada Y, Kano MR, Miyazono K, Uesaka M, Nishiyama N, Kataoka K. 2011. Accumulation of sub-100 nm polymeric micelles in poorly permeable tumours depends on size. Nat Nanotechnol 6:815–823.
18. Matsushita S, Chuang VT, Kanazawa M, Tanase S, Kawai K, Maruyama T, Suenaga A, Otagiri M. 2006. Recombinant human serum albumin dimer has high blood circulation activity and low vascular permeability in comparison with native human serum albumin. Pharm Res 23:882–891.
19. Chen RF. 1967. Removal of fatty acids from serum albumin by charcoal treatment. J Biol Chem 242:173–181.
20. Abuchowski A, van Es T, Palczuk NC, Davis FF. 1977. Alteration of immunological properties of bovine serum albumin by covalent attachment of polyethylene glycol. J Biol Chem 252:3578–3581.
21. Ishima Y, Sawa T, Kragh-Hansen U, Miyamoto Y, Matsushita S, Akaike T, Otagiri M. 2007. S-nitrosylation of human variant albumin Liprizzi (R410C) confers potent antibacterial and cytoprotective properties. J Pharmacol Exp Ther 320:969–977.
22. Yamaoka K, Tanigawara Y, Nakagawa T, Uno T. 1981. A pharmacokinetic analysis program (multi) for microcomputer. J Pharmacobiodyn 4:879–885.
23. Akaike T. 2000. Mechanisms of biological S-nitrosation and its measurement. Free Radic Res 33:461–469.

EPR 効果に基づくポリマー抗癌剤の腫瘍デリバリー

微小癌の検出・治療を目的としたセラノスティック薬剤の開発

中村　秀明[*1]・方　　軍[*2]・前　田　　浩[*3]

1．はじめに

　光照射により励起した光増感剤は，そのエネルギーを酸素分子に受け渡すことで，一重項酸素を発生する．一重項酸素は非常に反応性に富む活性酸素の一つであり，近傍の物質に酸化損傷を与える．そのため，光増感剤を癌組織に集積させた後に，癌組織に光を照射することで，その局所のみに一重項酸素を発生させ，癌組織選択的に酸化傷害を与えることが可能となり，癌治療を行うことができる．この癌治療法を光線力学的療法（PDT, photodynamic therapy）と呼び，わが国においては早期肺癌（0期または1期）および腫瘍摘出手術施行時の原発性悪性脳腫瘍に対して承認されている．光増感剤としてはポルフィリン系の薬剤が最も知られており，2014年現在，日本では，フォトフリン®（ポルフィマーナトリウム）およびレザフィリン®（タラポルフィンナトリウム）が，癌の光線力学的療法剤として認可，使用されている．しかし，投与後2週間は直射日光を避けるなど，光線過敏症を予防する措置が取られているのが現状であり，この問題はフォトフリンおよびレザフィリンなどの薬物動態の悪さに起因すると

ころが多い．つまり，薬剤が皮膚へ分布するため，直射日光などにより紅斑，水泡等の光線過敏反応を引き起こす恐れがあり，改善が望まれている．

　ドラッグデリバリーサイエンス（DDS）研究は，薬物の体内動態の把握やメカニズムの解析，さらにその改善を目的とした研究であり，薬物そのものの改変によって，その動態に起因する問題を解決する研究分野である．例えば，癌治療におけるDDSの第一問題としては，松村・前田等の提唱した enhanced permeability and retention（EPR）効果の問題が挙げられる[1]．つまり，血中に投与された薬物が，組織への漏出性の亢進，ならびにリンパ系の機能不全による組織からの排除不全によって，より癌組織に持続的に滞留することができる．ただしその薬物は高分子型の抗癌剤（>40 kDa）であることが必要である．つまり，癌組織に選択的に薬物が集積する現象がEPR効果であり，それを利用したものである．光増感剤も高分子化すればEPR効果により，皮膚などの正常組織への分布が抑制され，癌組織に選択的に集積する．そのため，光線過敏症などの副作用の軽減のみならず，組織傷害の腫瘍選択性など治療効果の増強につながる．また，ポルフィリン系化合物を代表とする光増感剤の多くは，光照射により一重項酸素と蛍光を効率よく発する性質を持つため，癌組織に高濃度に集積させることで，蛍光を利用した癌組織の検出につなげること

[*1] Hideaki Nakamura　崇城大学DDS研究所　薬学部微生物学研究室　助教　博士（薬学）
[*2] Jun Fang　同上　准教授　博士（医学）
[*3] Hiroshi Maeda　崇城大学DDS研究所　特任教授　博士（医学）
Micelles of Zinc Protoporphyrin Conjugated to HPMA Polymer for Imaging and Light-induced Antitumor Effect Based on the EPR Effect Driven Tumor Delivery